





Article

One Pot Ultrasonic Assisted $[\text{Ni}(\text{tptz})\text{Cl}(\text{H}_2\text{O})_2][\text{Ni}(\text{tptz})(\text{H}_2\text{O})_3]\cdot 3\text{Cl}\cdot 5\text{H}_2\text{O}$ Complex Formation Using Triazine Ligand, XRD/HSA-Interactions, and Spectral and Thermal Investigation

Abeer A. AlObaid ¹, Ahmed Boshala ² , Younis O. Ben Amer ³, Abraham F. Abraham ², Nabil Al-Zaqri ¹ , Mohammed Suleiman ⁴, Abdelkader Zarrouk ⁵ , Nawaf Al-Maharik ⁶, Hussien A. Khamees ⁷ and Ismail Warad ^{8,*} 



Citation: AlObaid, A.A.; Boshala, A.; Ben Amer, Y.O.; Abraham, A.F.; Al-Zaqri, N.; Suleiman, M.; Zarrouk, A.; Al-Maharik, N.; Khamees, H.A.; Warad, I. One Pot Ultrasonic Assisted $[\text{Ni}(\text{tptz})\text{Cl}(\text{H}_2\text{O})_2][\text{Ni}(\text{tptz})(\text{H}_2\text{O})_3]\cdot 3\text{Cl}\cdot 5\text{H}_2\text{O}$ Complex Formation Using Triazine Ligand, XRD/HSA-Interactions, and Spectral and Thermal Investigation. *Crystals* **2021**, *11*, 1474. <https://doi.org/10.3390/cryst11121474>

Academic Editors: Assem Barakat and Alexander S. Novikov

Received: 27 October 2021

Accepted: 23 November 2021

Published: 27 November 2021

Publisher's Note: MDPI stays neutral with regard to jurisdictional claims in published maps and institutional affiliations.



Copyright: © 2021 by the authors. Licensee MDPI, Basel, Switzerland. This article is an open access article distributed under the terms and conditions of the Creative Commons Attribution (CC BY) license (<https://creativecommons.org/licenses/by/4.0/>).

- 1 Department of Chemistry, College of Science, King Saud University, P.O. Box 2455, Riyadh 11451, Saudi Arabia; aalobaid@ksu.edu.sa (A.A.A.); nalzaqri@ksu.edu.sa (N.A.-Z.)
 - 2 Libyan authority for Scientific Research, Tripoli P.O. Box 80045, Libya; ahmedboshala@yahoo.co.uk (A.B.); abrahamff@hotmail.com (A.F.A.)
 - 3 Chemistry Department, Faculty of Science, Benghazi University, Benghazi P.O. Box 1308, Libya; dean.sci@uob.edu.ly
 - 4 Department of Chemistry, Science College, An-Najah National University, Nablus P.O. Box 7, Palestine; m.suliman@najah.edu
 - 5 Laboratory of Materials, Nanotechnology and Environment, Faculty of Sciences, Mohammed V University in Rabat, Agdal-Rabat, P.O. Box 1014, Rabat 11000, Morocco; azarrouk@gmail.com
 - 6 School of Chemistry, Biomedical Sciences Research Complex, University of St Andrews, North Haugh, St Andrews KY16 9ST, UK; na10@st-andrews.ac.uk
 - 7 Department of Medical Science, Community College—Abs, Abs P.O. Box 1, Yemen; h_khamees36@yahoo.com
 - 8 Department of Chemistry and Earth Sciences, College of Arts and Sciences, Qatar University, Doha P.O. Box 2713, Qatar
- * Correspondence: ismail.warad@qu.edu.qa

Abstract: Under room temperature ultrasonic conditions, mixing the neutral 2,4,6-tri(pyridin-2-yl)-1,3,5-triazine (tptz) ligand with Ni(II) salt resulted in the preparation of a unique $[\text{Ni}(\text{tptz})\text{Cl}(\text{H}_2\text{O})_2][\text{Ni}(\text{tptz})(\text{H}_2\text{O})_3]\cdot 3\text{Cl}\cdot 5\text{H}_2\text{O}$ complex with two different nickel(II) centers in a high yield. The crystal structure of $[\text{Ni}(\text{tptz})\text{Cl}(\text{H}_2\text{O})_2][\text{Ni}(\text{tptz})(\text{H}_2\text{O})_3]\cdot 3\text{Cl}\cdot 5\text{H}_2\text{O}$ revealed the existence of distorted octahedral around both Ni(II) centers. The complex structure was further supported by FT-IR, UV-Vis., CHN-EA, TGA and EDX. The computed HSA was also performed to support the XRD interaction types. The existence of the H_2O molecules in the crystal lattice was examined by FT-IR and TG/DTG measurements that proved the presence of coordinated and uncoordinated water molecules. Moreover, the thermal stability of the desired complex was evaluated at open atmosphere via TG/DTG and showed stability up to $\sim 400^\circ\text{C}$ and multistep thermal decomposition.

Keywords: spectral; Ni(II) complex; tptz ligand; crystal structure

1. Introduction

In recent years, there has been a rising advantage in experimental and theoretical research directed to 2,4,6-tri(pyridin-2-yl)-1,3,5-triazine (tptz) and its derivatives [1–5]. Non-covalent interactions, such as stacking and H-bonding play significant roles in the process of crystallization [6–12]. Moreover, the 2,4,6-tri-2-pyridyl-1,3,5-triazine is considered to be a stable bidentate and tridentate ligand, therefore, it is interesting to study its coordination mode, especially by using different metal centers [8,13,14]. Tptz ligand has the potential to be utilized as an excellent chelating analytical reagent to detect traces of ionic metals via chromatic complexation process [8–14].

Tptz complexes denoted promising applications in several research areas such as in the catalysis of many organic reactions [13–15], solar energy and emitting devices [16–18].

Moreover, many transition metals of tptz complexes such as Os(II), Ru(II) Cu(II) and Pt(II), were found to have very promising biological aspects such as being antitumor, antibacterial and antifungal [19–28].

In the present study, the double 1:1 co-crystallized nickel(II) centers complex with neutral 2,4,6-tri(pyridin-2-yl)-1,3,5-triazine ligand was used to form $\{[\text{Ni}(\text{tptz})\text{Cl}(\text{H}_2\text{O})_2][\text{Ni}(\text{tptz})(\text{H}_2\text{O})_3]\}3\text{Cl}\cdot 5\text{H}_2\text{O}$ moiety matrix, $[\text{Ni}(\text{tptz})\text{Cl}(\text{H}_2\text{O})_2]$ and $[\text{Ni}(\text{tptz})(\text{H}_2\text{O})_3]$ complexes have been reported separately. Application of the ultrasonic medium in the reacting of nickel(II) chloride hexahydrate salt with commercial tptz ligand enabled the generation of $\{[\text{Ni}(\text{tptz})\text{Cl}(\text{H}_2\text{O})_2][\text{Ni}(\text{tptz})(\text{H}_2\text{O})_3]\}3\text{Cl}\cdot 5\text{H}_2\text{O}$ complexes in one matrix. The designated ligand synthesis process was monitored by EDX, UV-vis. and FT-IR. Moreover, the interactions in the complex lattice figured out experimentally via XRD were computed by HSA analysis. Additionally, the thermal stability of $\{[\text{Ni}(\text{tptz})\text{Cl}(\text{H}_2\text{O})_2][\text{Ni}(\text{tptz})(\text{H}_2\text{O})_3]\}3\text{Cl}\cdot 5\text{H}_2\text{O}$ was examined by TG/DTG. The catalytic activity of the desired complex for oxidation of some organic compounds such as alcohol to produce carbonyls will be evaluated in future work.

2. Experimental Section

2.1. Measurements

All the chemicals and solvents were of reagent grade and used without further purification. Chemicals such as Nickel(II) chloride hexahydrate salt and 2,4,6-tri(pyridin-2-yl)-1,3,5-triazine were purchased from Fluka Switzerland. UV-Vis. measurements were performed in methanol solvent using TU-1901 double-beam spectrophotometer (Purkinje General Instrument Co., Ltd., Beijing, China). The FT-IR (MID. 4000–200 cm^{-1}) was recorded in solid state using PerkinElmer Spectrum 1000 FT-IR Spectrometer (PerkinElmer Inc., Waltham, MA, USA). MS data collection was carried out on a 711A (8 kV) Finnigan (PerkinElmer Inc., Waltham, MA, USA). CHN-analysis was performed using Elementar-Vario EL-analyzer (PerkinElmer Inc., Waltham, MA, USA). SEM-EDX were performed on NovaNano™ SEM 450 FEI (Bruker GmbH, Berlin, Germany). Ultrasonic generators were carried out on an Ultrasonic PP SONICA-2200 EP (SOLTEC Srl, Milano, Italy), input: 50–60 Hz/305 W, the rod was immersed in the reaction mixture and pulsed for 10 s, then rested for 20 s, ongoing for 5 min, which was enough to turn the color of reaction mixture to brown, a sign that the complexation reaction is completed; therefore, no sufficient increase in the temperature was noted.

2.2. Computational Crystal Data

The CIF file crystallographic data was taken as reference for the calculation when HSA was performed using the CRYSTAL EXPLORER 3.1 [29].

Data collection was performed on a Bruker-AXS-SMART APEX CCD diffractometer using Mo-K α radiation ($\lambda = 0.71073 \text{ \AA}$) at 130(2) K. The structures were solved by direct method using SIR-92 and refined by full-matrix least squares [30]. Non hydrogen bond atoms were refined anisotropically using SHELXL [31]. Hydrogen atoms were located geometrically and refined isotropically. Crystal data and details of refinements of the structures reported as in Table 1.

2.3. Synthesis of the $\{[\text{Ni}(\text{tptz})\text{Cl}(\text{H}_2\text{O})_2][\text{Ni}(\text{tptz})(\text{H}_2\text{O})_3]\}3\text{Cl}\cdot 5\text{H}_2\text{O}$ Complex

To a solution of 2,4,6-tri(2pyridin-2-yl)-1,3,5-triazine (0.312 g, 1.0 mmol) in 30 mL of ethanol/water, $\text{NiCl}_2\cdot 6\text{H}_2\text{O}$ (0.238 g, 1.0 mmol) was added slowly. The mixture was kept under ultrasonic vibration reflux for further four hours. The formed greenish precipitate was separated by filtration and washed with ethanol and dried under vacuum (0.82 g with 78.82% yield), suitable pretty crystals were collected of equal molar equivalent by slow evaporation of chloroform for three weeks.

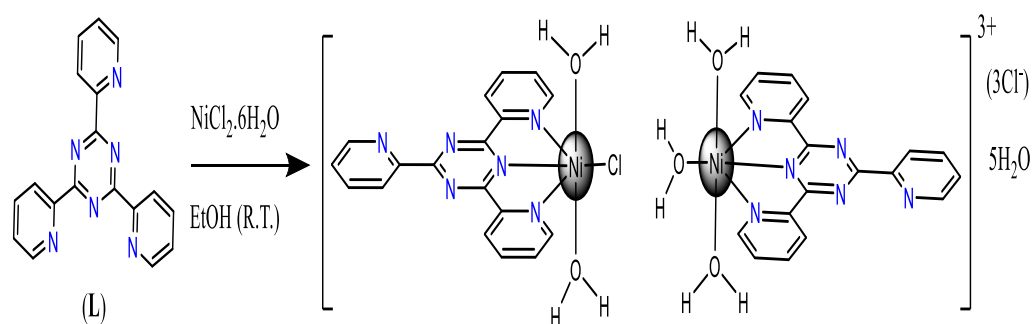
Table 1. Exp. XRD data of $[\text{Ni}(\text{tptz})\text{Cl}(\text{H}_2\text{O})_2][\text{Ni}(\text{tptz})(\text{H}_2\text{O})_3]3\text{Cl}\cdot 5\text{H}_2\text{O}$.

Empirical Formula	$\text{C}_{36}\text{H}_{44}\text{Cl}_4\text{N}_{12}\text{Ni}_2\text{O}_{10}$
CCDC	1,497,101
Formula weight	1064.05
Temperature	130(2) K
Wavelength	0.71073 Å
Crystal system	Monoclinic
Space group	P2(1)/n
Unit cell dimensions	a = 17.139(2) Å b = 14.6181(19) Å c = 17.983(2) Å $\beta = 95.576(4)^\circ$
Volume	4484.2(10) Å ³
Z	4
Density (calculated)	1.576 mg/m ³
Absorption coefficient	1.147 mm ⁻¹
F(000)	2192
Crystal size	0.22 × 0.18 × 0.14 mm ³
Theta range for data collection	1.57 to 27.88°
Reflections collected	37,446
Independent reflections	699 [R(int) = 0.0835]
Completeness to theta = 27.88°	0.999
Absorption correction	Semi-empirical from equivalents
Max. and min. transmission	0.8560 and 0.7865
Refinement method	Full-matrix least squares on F ²
Data/restraints/parameters	10,699/30/657
Goodness-of-fit on F ²	0.725
Final R indices [I > 2 sigma(I)]	R ₁ = 0.00427, wR ₂ = 0.028
Largest diff. peak and hole	1.071 and -0.476 e.Å ⁻³

3. Results and Discussion

3.1. Synthesis, CHN-Analysis, EDX and SEM

The $[\text{Ni}(\text{tptz})\text{Cl}(\text{H}_2\text{O})_2][\text{Ni}(\text{tptz})(\text{H}_2\text{O})_3]3\text{Cl}\cdot 5\text{H}_2\text{O}$ complex was prepared by combining equal molar equivalent of the 2,4,6-tri(pyridin-2-yl)-1,3,5-triazine and $\text{NiCl}_2\cdot 4\text{H}_2\text{O}$ in water solution under ultrasonic vibration reflux conditions, as shown in Scheme 1. The complex was isolated as a greenish powder with mono and dictation Ni(II) centers resulting in a water-soluble complex formation.

**Scheme 1.** $[\text{Ni}(\text{tptz})\text{Cl}(\text{H}_2\text{O})_2][\text{Ni}(\text{tptz})(\text{H}_2\text{O})_3]3\text{Cl}\cdot 5\text{H}_2\text{O}$ complex synthesis.

The elemental analysis was confirmed by CHN-EA, shown as C, 40.64; H, 4.17 and N, 15.80%, composed to be C, 40.41; H, 4.27; N, 15.63% from $\text{C}_{36}\text{H}_{44}\text{Cl}_4\text{N}_{12}\text{Ni}_2\text{O}_{10}$ formula with $[\text{Ni}(\text{tptz})\text{Cl}(\text{H}_2\text{O})_2][\text{Ni}(\text{tptz})(\text{H}_2\text{O})_3]3\text{Cl}\cdot 5\text{H}_2\text{O}$. EDX was used to confirm the atomic content of the complex, as seen in Figure 1. Only Ni, N, O, C and Cl peaks were recorded in EDX, which reflected the purity, the atomic content credibility and accuracy of the desired complex; these have been illustrated in Figure 1a. The external morphology and the purity

of the desired complexes were also evaluated by SEM analysis. Figure 1b shows a high degree of crystallization with semi-structured sheets and rods shapes.

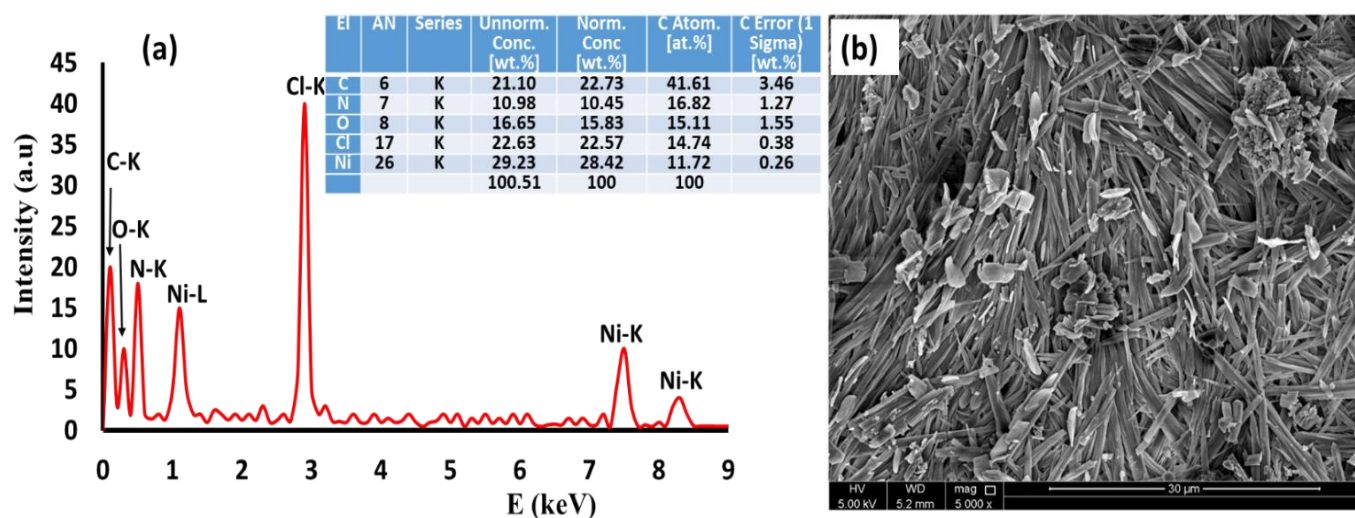


Figure 1. (a) EDX and (b) SEM (μm) of $\{[\text{Ni}(\text{tptz})\text{Cl}(\text{H}_2\text{O})_2][\text{Ni}(\text{tptz})(\text{H}_2\text{O})_3]\}3\text{Cl}\cdot 5\text{H}_2\text{O}$ complex.

3.2. XRD-Investigations

To ensure the crystal quality, color and purity, an image for the $\{[\text{Ni}(\text{tptz})\text{Cl}(\text{H}_2\text{O})_2][\text{Ni}(\text{tptz})(\text{H}_2\text{O})_3]\}3\text{Cl}\cdot 5\text{H}_2\text{O}$ complex, together with the single crystal XRD pattern, were performed and inserted in Figure 2a,b, respectively. The pure yellow single color and the multi-peaks of single crystal XRD result reflected the well-defined crystalline peaks, indicating that the tptz ligand was successfully coordinated to Ni(II) center; moreover, such coordination mode behavior encouraged the complex crystallization in a good quality and high purity form, as can be seen in Figure 2. On another hand, the ORTEP of $\{[\text{Ni}(\text{tptz})\text{Cl}(\text{H}_2\text{O})_2][\text{Ni}(\text{tptz})(\text{H}_2\text{O})_3]\}3\text{Cl}\cdot 5\text{H}_2\text{O}$ and selected structural parameters are illustrated in Figure 2c and Table 2, respectively. The crystal structure of $\text{C}_{36}\text{H}_{44}\text{Cl}_4\text{N}_{12}\text{Ni}_2\text{O}_{10}$ is a monoclinic system with $\text{P2}(1)/n$ space group (Figure 2d).

The desired $\{[\text{Ni}(\text{tptz})\text{Cl}(\text{H}_2\text{O})_2][\text{Ni}(\text{tptz})(\text{H}_2\text{O})_3]\}3\text{Cl}\cdot 5\text{H}_2\text{O}$ was co-crystallized in one-to-one two-type Ni-complexes: one showing Ni with three water molecules and the one tptz ligand (**A**-form), and the other showing Ni with two water, one Cl and one tptz ligand (**B**-form). Additionally, there are three Cl counter anions and five water molecules detected per asymmetric unit. In both **A**- and **B**-forms, a destroyed octahedral geometry around the Ni(II) centers was detected; moreover, the structure Ni(II) centers were coordinated to the tptz via a tridentate N-mode of coordination, to 2N via pyridyl rings and to 1N via a triazine ring. In **A**-form, the other three coordinations were saturated via three water molecules; meanwhile, in **B**-form, one water molecule was replaced by one Cl ligand only two water molecules were coordinated to the Ni(II) center.

There were several classical short contacts H-bonds such as $\text{HO}-\text{H} \dots \text{Cl}$ with 2.254–2.360 Å, $\text{HO}-\text{H} \dots \text{O}_{\text{Water}}$ with 2.023–2.468 Å, non-classical $\text{C}-\text{H} \dots \text{Cl}$ with 2.860–2.810 Å, and $\text{C}-\text{H} \dots \text{O}_{\text{Water}}$ with 2.530–2.670 Å (Figure 2d).

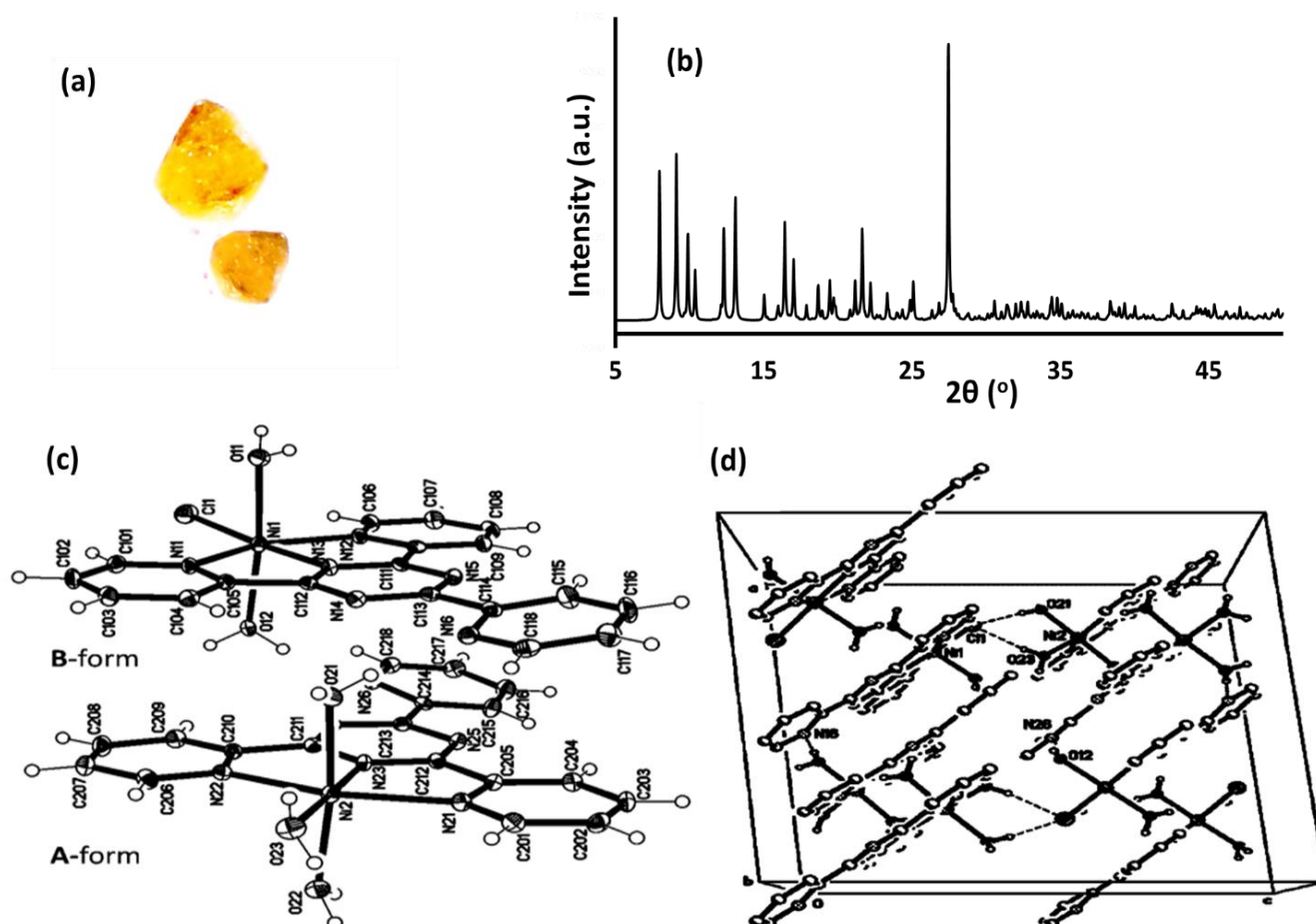


Figure 2. (a) Normal crystals image, (b) single crystal XRD pattern, (c) ORTEP and (d) packing diagrams of $[[\text{Ni}(\text{tptz})\text{Cl}(\text{H}_2\text{O})_2][\text{Ni}(\text{tptz})(\text{H}_2\text{O})_3]]3\text{Cl}\cdot 5\text{H}_2\text{O}$.

Table 2. Experimental XRD-bonds and angles values.

Bond Type	Bond Length (Å)	Angles Type	Angle Value (°)	Angles Type	Angle Value (°)
Ni(1)-N(13)	2.000(2)	N(13)-Ni(1)-O(11)	90.27(10)	N(12)-C(110)-C(111)	114.1(3)
Ni(1)-O(11)	2.056(3)	N(13)-Ni(1)-O(12)	92.90(10)	C(109)-C(110)-C(111)	122.2(3)
Ni(1)-O(12)	2.072(2)	O(11)-Ni(1)-O(12)	174.40(11)	N(15)-C(111)-N(13)	123.8(3)
Ni(1)-N(11)	2.164(3)	N(13)-Ni(1)-N(11)	76.30(10)	N(15)-C(111)-C(110)	121.7(3)
Ni(1)-N(12)	2.189(3)	O(11)-Ni(1)-N(11)	87.51(10)	N(13)-C(111)-C(110)	114.6(3)
Ni(1)-Cl(1)	2.3792(9)	O(12)-Ni(1)-N(11)	88.76(10)	N(13)-C(112)-N(14)	124.1(3)
Ni(2)-N(23)	1.988(2)	N(13)-Ni(1)-N(12)	76.15(10)	N(13)-C(112)-C(105)	114.2(3)
Ni(2)-O(23)	2.038(2)	O(11)-Ni(1)-N(12)	93.47(10)	N(14)-C(112)-C(105)	121.8(3)
Ni(2)-O(22)	2.047(2)	O(12)-Ni(1)-N(12)	91.76(10)	N(14)-C(113)-N(15)	125.9(3)
Ni(2)-O(21)	2.078(3)	N(11)-Ni(1)-N(12)	152.43(10)	N(14)-C(113)-C(114)	118.2(3)
Ni(2)-N(22)	2.146(3)	N(13)-Ni(1)-Cl(1)	175.97(8)	N(15)-C(113)-C(114)	116.0(3)
Ni(2)-N(21)	2.181(3)	O(11)-Ni(1)-Cl(1)	87.70(7)	N(16)-C(114)-C(115)	123.1(3)
N(11)-C(101)	1.331(4)	O(12)-Ni(1)-Cl(1)	89.41(7)	N(16)-C(114)-C(113)	116.2(3)
N(11)-C(105)	1.356(4)	N(11)-Ni(1)-Cl(1)	107.08(7)	C(115)-C(114)-C(113)	120.7(3)
N(12)-C(106)	1.332(4)	N(12)-Ni(1)-Cl(1)	100.48(7)	C(114)-C(115)-C(116)	118.3(3)
N(12)-C(110)	1.360(4)	N(23)-Ni(2)-O(23)	178.94(11)	C(117)-C(116)-C(115)	119.6(3)
N(13)-C(112)	1.324(4)	N(23)-Ni(2)-O(22)	94.06(10)	C(116)-C(117)-C(118)	118.1(3)
N(13)-C(111)	1.338(4)	O(23)-Ni(2)-O(22)	86.15(11)	N(16)-C(118)-C(117)	123.6(3)
N(14)-C(112)	1.335(4)	N(23)-Ni(2)-O(21)	91.83(10)	N(21)-C(201)-C(202)	123.0(3)
N(14)-C(113)	1.348(4)	O(23)-Ni(2)-O(21)	87.86(11)	C(203)-C(202)-C(201)	119.2(3)
N(15)-C(111)	1.328(4)	O(22)-Ni(2)-O(21)	172.09(11)	C(202)-C(203)-C(204)	119.0(3)
N(15)-C(113)	1.347(4)	N(23)-Ni(2)-N(22)	76.92(10)	C(205)-C(204)-C(203)	118.4(3)

Table 2. Cont.

Bond Type	Bond Length (Å)	Angles Type	Angle Value (°)	Angles Type	Angle Value (°)
N(16)-C(118)	1.334(4)	O(23)-Ni(2)-N(22)	102.05(11)	N(21)-C(205)-C(204)	123.5(3)
N(16)-C(114)	1.352(4)	O(22)-Ni(2)-N(22)	88.00(10)	N(21)-C(205)-C(212)	114.1(3)
N(21)-C(201)	1.337(4)	O(21)-Ni(2)-N(22)	88.19(10)	C(204)-C(205)-C(212)	122.4(3)
N(21)-C(205)	1.364(4)	N(23)-Ni(2)-N(21)	76.26(10)	N(22)-C(206)-C(207)	122.7(3)
N(22)-C(206)	1.338(4)	O(23)-Ni(2)-N(21)	104.77(10)	C(208)-C(207)-C(206)	119.2(3)
N(22)-C(210)	1.358(4)	O(22)-Ni(2)-N(21)	92.66(10)	C(207)-C(208)-C(209)	119.1(3)
N(23)-C(212)	1.333(4)	O(21)-Ni(2)-N(21)	93.87(10)	C(210)-C(209)-C(208)	118.2(3)
N(23)-C(211)	1.334(4)	N(22)-Ni(2)-N(21)	153.15(10)	N(22)-C(210)-C(209)	123.5(3)
N(24)-C(211)	1.329(4)	C(101)-N(11)-C(105)	117.7(3)	N(22)-C(210)-C(211)	113.9(3)
N(24)-C(213)	1.344(4)	C(101)-N(11)-Ni(1)	128.1(2)	C(209)-C(210)-C(211)	122.6(3)
N(25)-C(212)	1.325(4)	C(105)-N(11)-Ni(1)	114.2(2)	N(24)-C(211)-N(23)	123.7(3)
N(25)-C(213)	1.349(4)	C(106)-N(12)-C(110)	117.4(3)	N(24)-C(211)-C(210)	122.3(3)
N(26)-C(218)	1.337(4)	C(106)-N(12)-Ni(1)	128.6(2)	N(23)-C(211)-C(210)	114.0(3)
N(26)-C(214)	1.349(4)	C(110)-N(12)-Ni(1)	114.0(2)	N(25)-C(212)-N(23)	123.9(3)
C(101)-C(102)	1.386(4)	C(112)-N(13)-C(111)	117.5(3)	N(25)-C(212)-C(205)	122.1(3)
C(102)-C(103)	1.377(4)	C(112)-N(13)-Ni(1)	121.2(2)	N(23)-C(212)-C(205)	114.0(3)
C(103)-C(104)	1.385(4)	C(111)-N(13)-Ni(1)	121.1(2)	N(24)-C(213)-N(25)	125.5(3)
C(104)-C(105)	1.383(4)	C(112)-N(14)-C(113)	114.2(3)	N(24)-C(213)-C(214)	118.0(3)
C(105)-C(112)	1.480(4)	C(111)-N(15)-C(113)	114.5(3)	N(25)-C(213)-C(214)	116.4(3)
C(106)-C(107)	1.396(5)	C(118)-N(16)-C(114)	117.4(3)	N(26)-C(214)-C(215)	122.8(3)
C(107)-C(108)	1.370(4)	C(201)-N(21)-C(205)	117.0(3)	N(26)-C(214)-C(213)	116.4(3)
C(108)-C(109)	1.391(4)	C(201)-N(21)-Ni(2)	129.2(2)	C(215)-C(214)-C(213)	120.8(3)
C(109)-C(110)	1.383(4)	C(205)-N(21)-Ni(2)	113.8(2)	C(216)-C(215)-C(214)	118.5(3)
C(110)-C(111)	1.477(4)	C(206)-N(22)-C(210)	117.3(3)	C(217)-C(216)-C(215)	119.0(3)
C(113)-C(114)	1.489(4)	C(206)-N(22)-Ni(2)	128.4(2)	C(216)-C(217)-C(218)	118.9(3)
C(114)-C(115)	1.376(5)	C(210)-N(22)-Ni(2)	114.3(2)	N(26)-C(218)-C(217)	123.5(3)
C(115)-C(116)	1.391(4)	C(212)-N(23)-C(211)	117.3(3)		
C(116)-C(117)	1.378(5)	C(212)-N(23)-Ni(2)	121.9(2)		
C(117)-C(118)	1.386(5)	C(211)-N(23)-Ni(2)	120.8(2)		
C(201)-C(202)	1.389(4)	C(211)-N(24)-C(213)	114.8(3)		
C(202)-C(203)	1.378(4)	C(212)-N(25)-C(213)	114.7(3)		
C(203)-C(204)	1.391(4)	C(218)-N(26)-C(214)	117.3(3)		
C(204)-C(205)	1.376(4)	N(11)-C(101)-C(102)	122.7(3)		
C(205)-C(212)	1.479(4)	C(103)-C(102)-C(101)	119.1(3)		
C(206)-C(207)	1.384(4)	C(102)-C(103)-C(104)	119.3(3)		
C(207)-C(208)	1.382(4)	C(105)-C(104)-C(103)	118.0(3)		
C(208)-C(209)	1.385(4)	N(11)-C(105)-C(104)	123.1(3)		
C(209)-C(210)	1.379(4)	N(11)-C(105)-C(112)	114.1(3)		
C(210)-C(211)	1.481(4)	C(104)-C(105)-C(112)	122.8(3)		
C(213)-C(214)	1.483(4)	N(12)-C(106)-C(107)	122.2(3)		
C(214)-C(215)	1.390(4)	C(108)-C(107)-C(106)	119.8(3)		
C(215)-C(216)	1.385(4)	C(107)-C(108)-C(109)	119.2(3)		
C(216)-C(217)	1.376(4)	C(110)-C(109)-C(108)	117.7(3)		
C(217)-C(218)	1.377(4)	N(12)-C(110)-C(109)	123.7(3)		

3.3. HSA and 2D-FP

To learn more about the nature of bonding as short contacts between molecules in the complex crystal, the CIF file was subjected to HSA and 2D-FB analysis [32–44]. The presence of water molecules and chlorine anions linked or unrelated to the nickel center created many short connections that formed unique HSA 3D-artitures. The HSA computation results are demonstrated in Figure 3a with declarations of the d_{norm} , 2D-FP and shape index calculated in the range -0.578 to 1.486 a.u. Generally, the surface structure of $[\text{Ni}(\text{tptz})\text{Cl}(\text{H}_2\text{O})_2][\text{Ni}(\text{tptz})(\text{H}_2\text{O})_3]3\text{Cl}\cdot 5\text{H}_2\text{O}$ reflected the presence of 16 spots, only big red spots. The large red spots reflected a strong and short interaction consistent with three types of hydrogen bonds such as $\text{H} \dots \text{O}$, $\text{H} \dots \text{Cl}$ and $\text{H} \dots \text{N}$ with several lengths and unique three-dimensional H-bonds with only polar H of water molecules.

No small spots are detected since the proton in C-H is not polar-like enough with water protons. The shape index reflected the presence of the Cl, O and N nucleophilic sites (red) and 20 polar protons belongs to 10 water molecules as electrophile sites, indicated by the blue color on the shape index surface (Figure 3b). Moreover, the atom-to-atom two dimensional fingerprint (2D-FP) intermolecular percentage plot revealed the H...H 44.6% interaction with the largest percentage contribution; meanwhile, the H... Ni had the smallest percentage contribution at 0%, as shown in Figure 3c. The total 2D-FP H... Atoms ratios analysis were illustrated as the following H...H>Cl...H>O...H>C...H>N...H>Ni...H. The 2D-FP calculation results are consistent with the practical observations of the experimental XRD-measurements, as the presence of water molecules in the crystal lattice raised the H-interactions values, H... H and H... Cl, and H... O had the 2D-FP highest values; therefore, this can be seen to support the classical HO-H... .Cl and HO-H... .O_{Water}, and non-classical C-H... .Cl and C-H... .O_{Water} H-bonds formation. Moreover, since the ratio of the N... H was very small, the chance of forming HO-H... .N or C-H... .O hydrogen bonds is rare, and this is actually what the XRD has seen, as there are no such bonds that have been detected in the crystal lattice.

3.4. UV-Vis. and IR Investigation

The electronic absorption behavior of {[Ni(tptz)Cl(H₂O)₂][Ni(tptz)(H₂O)₃]}3Cl.5H₂O complex was performed in H₂O at RT. In the UV area, the tptz ligand part in the desired complex displayed the π to π^* , π to n and n to π^* absorption peaks, as can be seen at λ_{\max} values 235, 275, 315 and 355 nm in Figure 4a. Moreover, in the visible area, the octahedral d-to-d electrons transfer of Ni(II) centers were detected as broadband at λ_{\max} 418 nm and a weak band at 520 nm (Figure 4a).

FT-IR of the {[Ni(tptz)Cl(H₂O)₂][Ni(tptz)(H₂O)₃]}3Cl.5H₂O complex was recorded in the solid and is illustrated in Figure 4b and Table 3. FT-IR reflected the uncoordinated water molecular $\nu_{\text{O-H}}$ at 3440 cm^{-1} with broadband, the water coordinated molecular $\nu_{\text{O-H}}$ at 3290 cm^{-1} with a sharp peak and the $\nu_{\text{C-H}}$ peak at 3040 cm^{-1} signalized to triazine ligand C-H aromatic rings vibrations. The IR of the O-H bending band in water was detected at 1640 cm^{-1} , the $\nu_{\text{C=N}}$ band in tptz was recorded at a lower frequency $\sim 1510 \text{ cm}^{-1}$ confirming the C=N \rightarrow Ni(II) coordination bond formation; moreover, the Ni-N and Ni-O bonds formation were supported by bands at 450 and 550 cm^{-1} , respectively (Figure 5b).

Table 3. IR stretching vibrations (cm^{-1}) of main functional groups.

$\nu_{\text{HO-H}}$	$\nu_{\text{O-H}}$	$\nu_{\text{C-H}}$	$\nu_{\text{C=N}}$	$\nu_{\text{C=C}}$	$\nu_{\text{Ni-O}}$	$\nu_{\text{Ni-N}}$	$\nu_{\text{Ni-Cl}}$
3440	3290	3040	1510	1350	550	450	240

3.5. TGA Analysis

Thermogravimetric analysis TG/DTG of {[Ni(tptz)Cl(H₂O)₂][Ni(tptz)(H₂O)₃]}3Cl.5H₂O was performed in an open atmosphere (Figure 5) with a heat rate 2 °C/min [45,46]. The desired complex goes through four steps of decompositions as seen in Figure 5. In general, the desired complex showed high thermal stability, it is stable after losing water molecules up to 400 °C. The uncoordinated water molecule decayed at 80 °C with 8.5% and $T_{\text{DTG}} = 85 \text{ °C}$ to reach {[Ni(tptz)Cl(H₂O)₂][Ni(tptz)(H₂O)₃]}3Cl, meanwhile, the coordinated H₂O molecules were lost at 160 °C with 8.5 percentage and $T_{\text{DTG}} = 155 \text{ °C}$ to give {[Ni(tptz)Cl][Ni(tptz)]}3Cl. This is seen as total agreeing with the IR and XRD results, since five uncoordinated and five coordinated H₂O molecules were detected in the lattice of the crystal. The complex decayed in the third step in a complicated, very broad step starting from 410 °C and ending at 580 °C with $T_{\text{DTG}} = 450, 500$ and 550 °C, where all the organic content decomposed or de-structured away from the metallic center losing 58% weight percentage to produce a matrix without organic ligand [Ni₂Cl₄]. The [Ni₂Cl₄] matrix was decomposed in the fourth step in one complicated step (decomposition followed by oxidation), since the four chloride atoms were lost and one oxygen atom was combined to the nickel centers to produce nickel

oxide (NiO) with 11.2% weight lost at $T_{DTG} = 690$ °C temperature. The formation of nickel oxide was confirmed by IR, where the characteristic sign of Ni=O of the final product appeared at 465 nm.

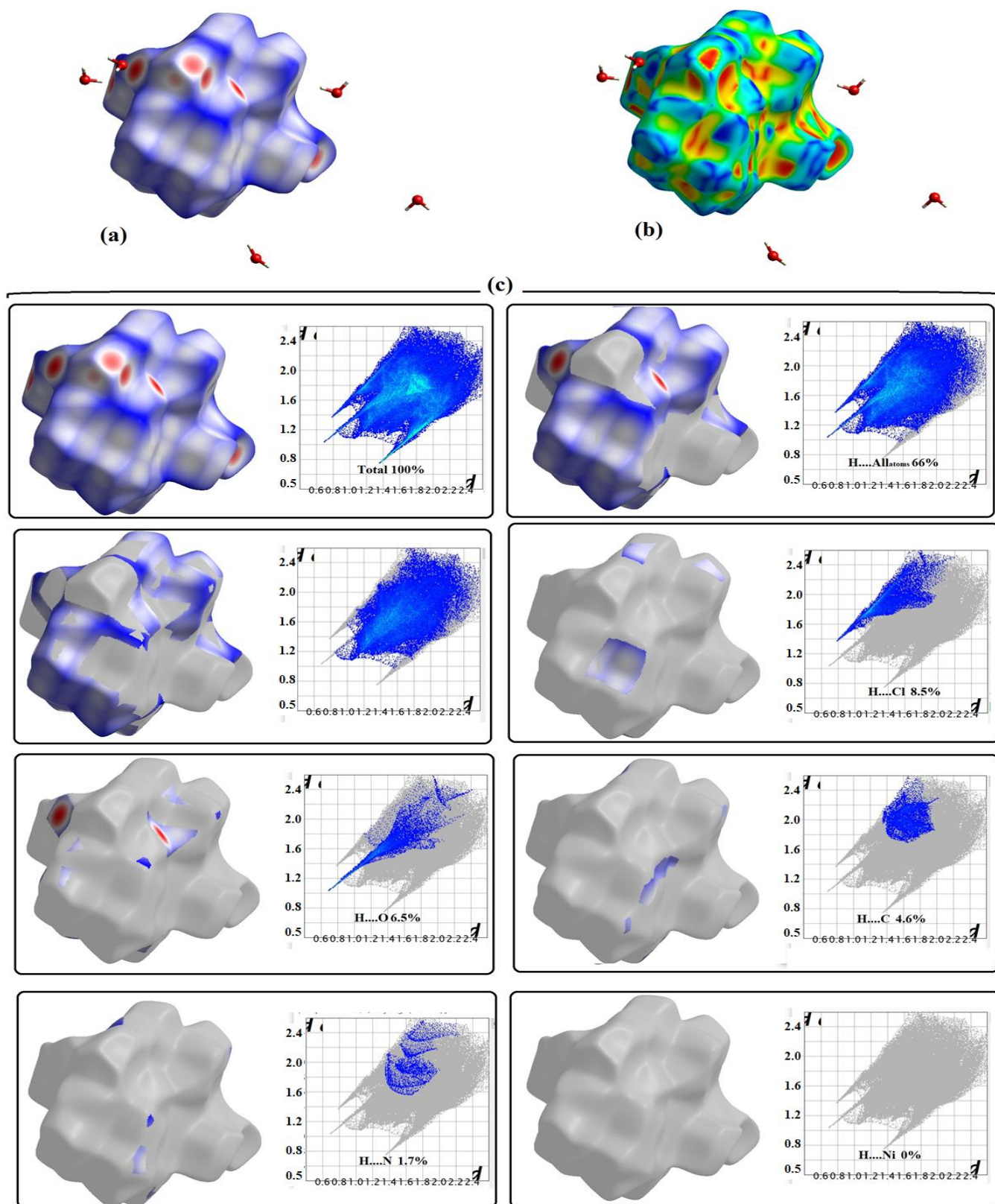


Figure 3. (a) d_{norm} , (b) shape index and (c) 2D-FP over the $[\text{Ni}(\text{tptz})\text{Cl}(\text{H}_2\text{O})_2][\text{Ni}(\text{tptz})(\text{H}_2\text{O})_3]3\text{Cl}\cdot 5\text{H}_2\text{O}$.

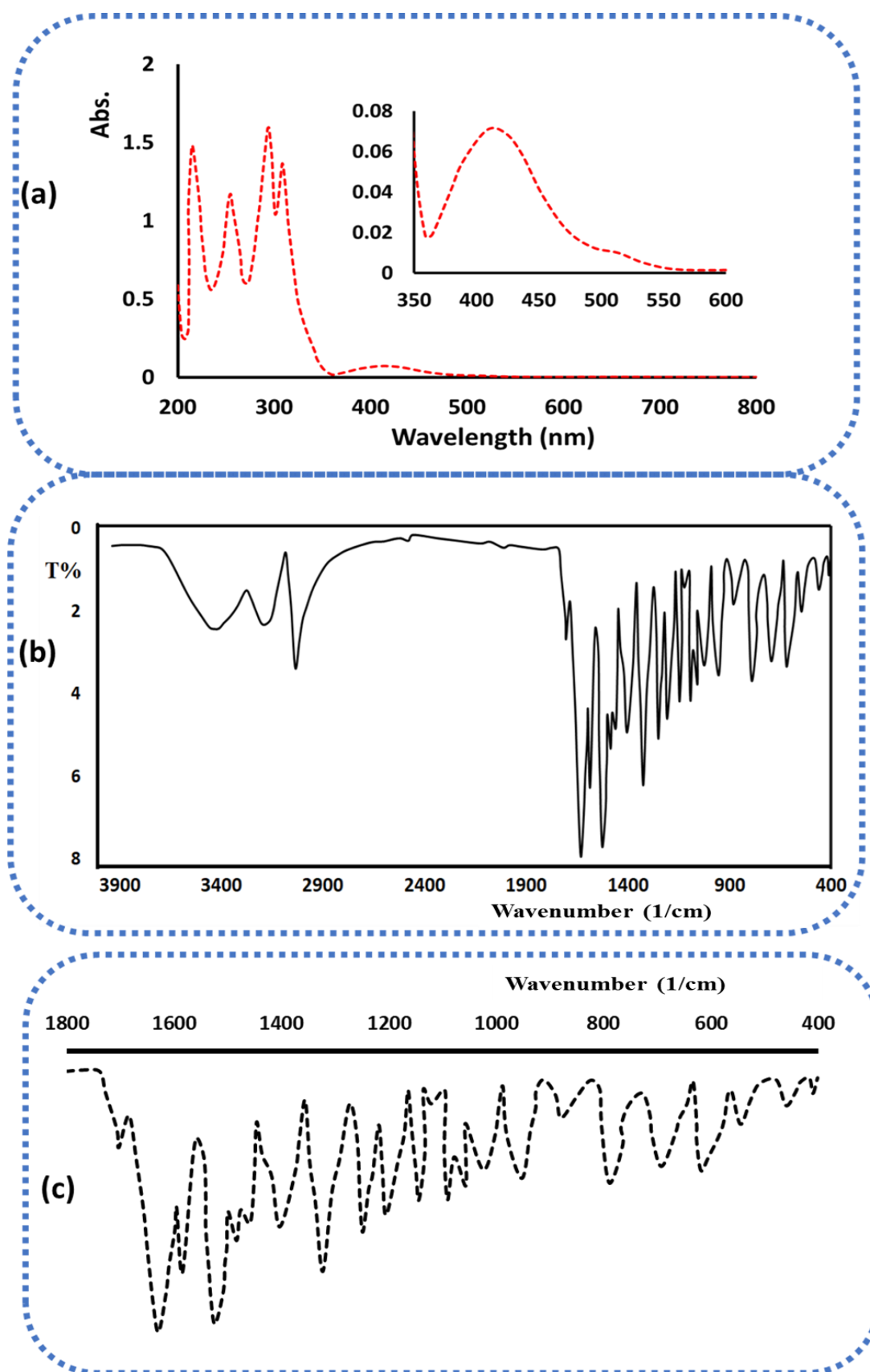


Figure 4. (a) UV-Vis. in water (b) Full scale and (c) 1800–400 cm^{-1} scale FT-IR of $[[NiCl(H_2O)_2][NiL(H_2O)_3]] \cdot 3Cl \cdot 5H_2O$.

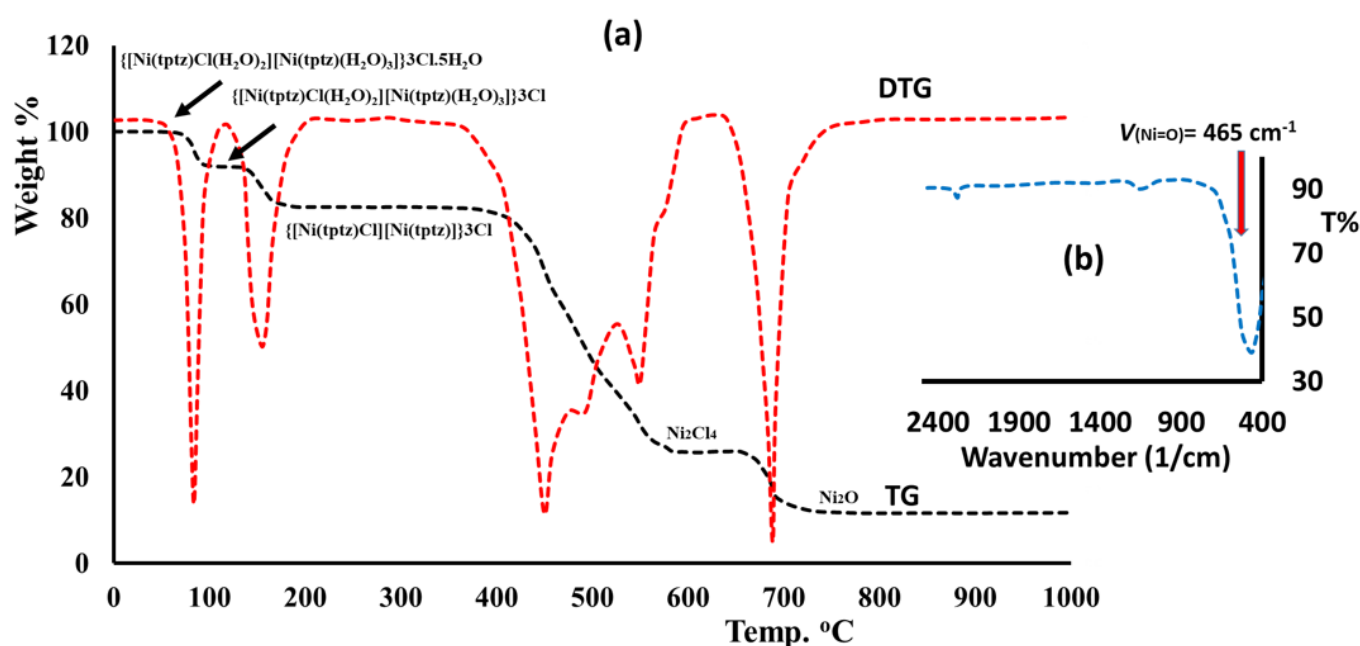


Figure 5. (a) TGA of the $\{[\text{Ni}(\text{tpz})\text{Cl}(\text{H}_2\text{O})_2][\text{Ni}(\text{tpz})(\text{H}_2\text{O})_3]\}3\text{Cl}\cdot 5\text{H}_2\text{O}$ and (b) $\text{Ni}=\text{O}$ IR of the final thermal product.

4. Conclusions

The ultrasonic aqueous medium for the preparation of $\{[\text{Ni}(\text{tpz})\text{Cl}(\text{H}_2\text{O})_2][\text{Ni}(\text{tpz})(\text{H}_2\text{O})_3]\}3\text{Cl}\cdot 5\text{H}_2\text{O}$ resulted in very good yield and one pot reaction. The octahedral structural geometry around both centers has been confirmed by 3D-structure XRD-result. In the crystal structure two different nickel(II) centers, chlorinated $\text{Ni}(\text{tpz})\text{Cl}(\text{H}_2\text{O})_2$ and non-chlorinated $\text{Ni}(\text{tpz})(\text{H}_2\text{O})_3$ unique complexes were reported in one matrix. The physicochemical structural analysis using FT-IR, UV-Vis., CHN-EA, XRD and EDX supported the atomic content of the $\{[\text{Ni}(\text{tpz})\text{Cl}(\text{H}_2\text{O})_2][\text{Ni}(\text{tpz})(\text{H}_2\text{O})_3]\}3\text{Cl}\cdot 5\text{H}_2\text{O}$. The XRD-experimental classical and non-classical H-bonds interactions such as $\text{HOH}\dots\text{Cl}$, $\text{HOH}\dots\text{O}$, $\text{CH}\dots\text{Cl}$, and $\text{CH}\dots\text{O}$ were successfully computed by HSA- and supported by TG/DTG analysis. The IR, CHN-EA and TG results are consistent with the XRD result in finding several coordinated and uncoordinated water molecules in the lattice of the desired complex. Moreover, the complex showed a multistep thermal breakdown, four steps are needed to reach to the NiO nickel oxide as a stable product.

Author Contributions: Formal analysis, A.A.A.; A.B.; Y.O.B.A.; N.A.-Z.; H.A.K. and A.F.A. Data curation, M.S.; Writing A.Z.; N.A.-M. and I.W. All authors have read and agreed to the published version of the manuscript.

Funding: The authors extend their appreciation to the Researchers Supporting Project number (RSP-2021/396), King Saud University, Riyadh, Saudi Arabia.

Data Availability Statement: Data is contained within the article.

Acknowledgments: The authors extend their sincere thanks to Ulrich Flörke Department Chemie, Universität Paderborn, Warburger Strasse 100, 33098 Paderborn, Germany for solving the crystal structure of the complex. Similar thanks go to the staff member at the Chemistry department, Faculty of Science, Benghazi University; Huda Muftah Sheppaek, Wjdan Omar Algezzeri, and Iman Mahmoud for their help to prepare the Schiff base, and special thanks go to Manchester salt and Catalysis Ltd., UK. The authors extend their appreciation to the Researchers Supporting Project number (RSP-2021/396), King Saud University, Riyadh, Saudi Arabia.

Conflicts of Interest: The authors declare no conflict of interest.

References

1. Barakat, A.; El-Faham, A.; Haukka, M.; Al-Majid, A.; Soliman, S. s-Triazine pincer ligands: Synthesis of their metalcomplexes, coordination behavior, and applications. *Appl. Organomet. Chem.* **2021**, *35*, e6317. [[CrossRef](#)]
2. Hadadzadeh, H.; Maghami, M.; Simpson, J.; Khalaji, A.; Abdi, K. Nickel(II) polypyridyl Complexes of 2,4,6-Tris(2-pyridyl)-1,3,5-triazine. *J. Chem. Crystallogr.* **2012**, *42*, 656–667. [[CrossRef](#)]
3. Cheng, D.-Y.; Xu, W.; Zheng, Y.-Q. Aquaoxalato (2,4,6-tri-2-pyridyl-1,3,5-triazine) cobalt (II) tetrahydrate. *Acta Crystallogr. Sect. E Struct. Rep. Online* **2006**, *62*, m2561–m2563. [[CrossRef](#)]
4. Soliman, S.; Lasri, J.; Haukka, M.; Elmarghany, A.; Al-Majid, A.; El-Faham, A.; Barakat, A. Synthesis, X-ray structure, Hirshfeld analysis, and DFT studies of a new Pd(II) complex with an anionic s-triazine NNO donor ligand. *J. Mol. Struct.* **2020**, *1217*, 128463–128472. [[CrossRef](#)]
5. Therrien, B. Coordination chemistry of 2,4,6-tri(pyridyl)-1,3,5-triazine ligands. *J. Organomet. Chem.* **2011**, *696*, 637–651. [[CrossRef](#)]
6. Stang, P.J.; Olenyuk, B. Self-assembly, symmetry, and molecular architecture: Coordination as the motif in the rational design of supramolecular metallacyclic polygons and polyhedra. *Acc. Chem. Res.* **1997**, *30*, 502–518. [[CrossRef](#)]
7. Glaser, T.; Lügger, T.; Fröhlich, R. Synthesis, Crystal Structures, and Magnetic Properties of a Mono-and a Dinuclear Copper (II) Complex of the 2,4,6-Tris (2-pyridyl)-1,3,5-triazine Ligand. *Eur. J. Inorg. Chem.* **2004**, *2004*, 394–400. [[CrossRef](#)]
8. Zibaseresht, R.; Hartshorn, R.M. The nickel (II)/2,4,6-tris (2-pyridyl)-1,3,5-triazine system: Synthesis and crystallographic characterization of a series of complexes. *Aust. J. Chem.* **2005**, *58*, 345–353. [[CrossRef](#)]
9. Zheng, Y.-Q.; Xu, W.; Lin, F.; Fang, G.-S. Syntheses and crystal structures of copper (II) complexes derived from 2,4,6-tris (2-pyridyl)-1,3,5-triazine. *J. Coord. Chem.* **2006**, *59*, 1825–1834. [[CrossRef](#)]
10. Xie, H.-Z.; Pan, W.-J. Aquaoxalato (2,4,6-tri-2-pyridyl-1,3,5-triazine) zinc (II) tetrahydrate. *Acta Crystallogr. Sect. E Struct. Rep. Online* **2007**, *63*, m1231–m1232. [[CrossRef](#)]
11. Witter, A.E.; Luther, G.W., III. Spectrophotometric measurement of seawater carbohydrate concentrations in neritic and oceanic waters from the US Middle Atlantic Bight and the Delaware estuary. *Mar. Chem.* **2002**, *77*, 143–156. [[CrossRef](#)]
12. Gupta, N.; Grover, N.; Neyhart, G.A.; Singh, P.; Thorp, H.H. Synthesis and properties of new DNA cleavage agents based on oxoruthenium (IV). *Inorg. Chem.* **1993**, *32*, 310–316. [[CrossRef](#)]
13. Ha, K. Dibromido (2,4,6-tri-2-pyridyl-1,3,5-triazine- κ^3N^2, N^1, N^6) manganese (II). *Acta Crystallogr. Sect. E Struct. Rep. Online* **2011**, *67*, m1655. [[CrossRef](#)] [[PubMed](#)]
14. Hadda, T.B.; Akkurt, M.; Baba, M.F.; Daoudi, M.; Bennani, B.; Kerbal, A.; Chohan, Z.H. Anti-tubercular activity of ruthenium (II) complexes with polypyridines. *J. Enzym. Inhib. Med. Chem.* **2009**, *24*, 457–463. [[CrossRef](#)] [[PubMed](#)]
15. Najafpour, M.M.; Holyńska, M.; Amini, M.; Kazemi, S.H.; Lis, T.; Bagherzadeh, M. Two new silver (I) complexes with 2,4,6-tris (2-pyridyl)-1,3,5-triazine (tptz): Preparation, characterization, crystal structure and alcohol oxidation activity in the presence of oxone. *Polyhedron* **2010**, *29*, 2837–2843. [[CrossRef](#)]
16. Sharma, S.; Chandra, M.; Pandey, D.S. New Multifunctional Complexes [Ru (κ^3 -L)(EPh₃)₂Cl]⁺[E = P, As; L = 2,4,6-Tris (2-pyridyl)-1,3,5-triazine] Containing both Group V and Polypyridyl Ligands. *Eur. J. Inorg. Chem.* **2004**, *2004*, 3555–3563. [[CrossRef](#)]
17. Kumar, P.; Singh, A.K.; Pandey, R.; Pandey, D.S. Bio-catalysts and catalysts based on ruthenium (II) polypyridyl complexes imparting diphenyl-(2-pyridyl)-phosphine as a co-ligand. *J. Organomet. Chem.* **2011**, *696*, 3454–3464. [[CrossRef](#)]
18. Dias, V.L.N.; Fernandes, E.N.; da Silva, L.M.S.; Marques, E.P.; Zhang, J.; Marques, A.L.B. Electrochemical reduction of oxygen and hydrogen peroxide catalyzed by a surface copper (II)-2,4,6-tris (2-pyridyl)-1,3,5-triazine complex adsorbed on a graphite electrode. *J. Power Sources* **2005**, *142*, 10–17. [[CrossRef](#)]
19. Li, S.; Zhang, L.; Kim, J.; Pan, M.; Shi, Z.; Zhang, J. Synthesis of carbon-supported binary FeCo–N non-noble metal electrocatalysts for the oxygen reduction reaction. *Electrochim. Acta* **2010**, *55*, 7346–7353. [[CrossRef](#)]
20. De Silva, C.R.; Li, F.; Huang, C.; Zheng, Z. Europium β -diketonates for red-emitting electroluminescent devices. *Thin Solid Film* **2008**, *517*, 957–962. [[CrossRef](#)]
21. Anandan, S.; Latha, S.; Murugesan, S.; Madhavan, J.; Muthuraaman, B.; Maruthamuthu, P. Synthesis, characterization and fabrication of solar cells making use of [Ru (dcbpy)(tptz) X] X (where X = Cl[−], SCN[−], CN[−]) complexes. *Sol. Energy* **2005**, *79*, 440–448. [[CrossRef](#)]
22. Rubino, S.; Portanova, P.; Albanese, A.; Calvaruso, G.; Orecchio, S.; Fontana, G.; Stocco, G.C. Mono-and polynuclear complexes of Pt (II) with polypyridyl ligands: Synthesis, spectroscopic and structural characterization and cytotoxic activity. *J. Inorg. Biochem.* **2007**, *101*, 1473–1482. [[CrossRef](#)] [[PubMed](#)]
23. Rubino, S.; Portanova, P.; Girasolo, A.; Calvaruso, G.; Orecchio, S.; Stocco, G.C. Synthetic, structural and biochemical studies of polynuclear platinum (II) complexes with heterocyclic ligands. *Eur. J. Med. Chem.* **2009**, *44*, 1041–1048. [[CrossRef](#)] [[PubMed](#)]
24. Singh, S.K.; Sharma, S.; Chandra, M.; Pandey, D.S. Helical racemate architecture based on osmium (II)-polypyridyl complexes: Synthesis and structural characterisation. *J. Organomet. Chem.* **2005**, *690*, 3105–3110. [[CrossRef](#)]
25. Patel, R.N.; Singh, N.; Shukla, K.K.; Gundla, V.L.N.; Chauhan, U.K. Synthesis, characterization and biological activity of ternary copper (II) complexes containing polypyridyl ligands. *Spectrochim. Acta Part A Mol. Biomol. Spectrosc.* **2006**, *63*, 21–26. [[CrossRef](#)] [[PubMed](#)]
26. Marzano, C.; Pellei, M.; Tisato, F.; Santini, C. Copper complexes as anticancer agents. *Anti-Cancer Agents Med. Chem.* **2009**, *9*, 185–211. [[CrossRef](#)] [[PubMed](#)]

27. Hindo, S.S.; Frezza, M.; Tomco, D.; Heeg, M.J.; Hryhorczuk, L.; McGarvey, B.R.; Dou, Q.P.; Verani, C.N. Metals in anticancer therapy: Copper (II) complexes as inhibitors of the 20S proteasome. *Eur. J. Med. Chem.* **2009**, *44*, 4353–4361. [[CrossRef](#)]
28. Patel, M.N.; Parmar, P.A.; Gandhi, D.S. Square pyramidal copper (II) complexes with fourth generation fluoroquinolone and neutral bidentate ligand: Structure, antibacterial, SOD mimic and DNA-interaction studies. *Bioorg. Med. Chem.* **2010**, *18*, 1227–1235. [[CrossRef](#)] [[PubMed](#)]
29. Turner, M.J.; McKinnon, J.J.; Wolff, S.K.; Grimwood, D.J.; Spackman, P.R.; Jayatilaka, D.; Spackman, M.A. *CrystalExplorer 17*; University of Western: Perth, Australia, 2017.
30. Burla, M.C.; Caliandro, R.; Camalli, M.; Carrozzini, B.; Cascarano, G.L.; De Caro, L.; Giacovazzo, C.; Polidori, G.; Spagna, R. SIR2004: An improved tool for crystal structure determination and refinement. *J. Appl. Cryst.* **2005**, *38*, 381–388. [[CrossRef](#)]
31. Sheldrick, G.M. *SHELX-97, Release 97-2*; University of Göttingen: Göttingen, Germany, 1998.
32. Guerraoui, A.; Djedouani, A.; Jeanneau, E.; Boumaza, A.; Alsalmeh, A.; Zarrouk, A.; Salih, K.S.M.; Warad, I. Crystal structure and spectral of new hydrazine-pyran-dione derivative: DFT enol-hydrazone tautomerization via zwitterionic intermediate, hirshfeld analysis and optical activity studies. *J. Mol. Struct.* **2020**, *1220*, 128728–128738. [[CrossRef](#)]
33. Tabti, S.; Djedouani, A.; Aggoun, D.; Warad, I.; Rahmouni, S.; Romdhane, S.; Fouzi, H. New Cu (II), Co (II) and Ni (II) complexes of chalcone derivatives: Synthesis, X-ray crystal structure, electrochemical properties and DFT computational studies. *J. Mol. Struct.* **2018**, *1155*, 11–20. [[CrossRef](#)]
34. Hema, M.K.; Karthik, C.S.; Warad, I.; Lokanath, N.K.; Zarrouk, A.; Kumara, K.; Pampa, K.J.; Mallu, P. Regular square planer bis-(4,4,4-trifluoro-1-(thiophen-2-yl)butane-1,3-dione)/copper(II) complex: Trans/cis-DFT isomerization, crystal structure, thermal, solvatochromism, hirshfeld surface and DNA-binding analysis. *J. Mol. Struct.* **2018**, *1157*, 69–77. [[CrossRef](#)]
35. Warad, I.; Musameh, S.; Badran, I.; Nassar, N.N.; Brandao, P.; Tavares, C.J.; Barakat, A. Synthesis, solvatochromism and crystal structure of trans-[Cu(Et₂NCH₂CH₂NH₂)₂·H₂O](NO₃)₂ complex: Experimental with DFT combination. *J. Mol. Struct.* **2017**, *11148*, 328–338. [[CrossRef](#)]
36. Aouad, M.R.; Messali, M.; Rezki, N.; Al-Zaqri, N.; Warad, I. Single proton intramigration in novel 4-phenyl-3-((4-phenyl-1H-1,2,3-triazol-1-yl)methyl)-1H-1,2,4-triazole-5(4H)-thione: XRD-crystal interactions, physicochemical, thermal, Hirshfeld surface, DFT realization of thiol/thione tautomerism. *J. Mol. Liq.* **2018**, *264*, 621–630. [[CrossRef](#)]
37. Badran, I.; Abdallah, L.; Mubarakeh, R.; Warad, I. Effect of alkyl derivation on the chemical and antibacterial properties of newly synthesized Cu(II)-diamine complexes. *Moroc. J. Chem.* **2019**, *7*, 161–170.
38. Hema, M.K.; Karthik, C.S.; Lokanath, N.K.; Mallu, P.; Zarrouk, A.; Salih, K.S.M.; Warad, I. Synthesis of novel Cubane [Ni₄(ONO)₄(OCH₃)₄(OOH)₄] cluster: XRD/HSA-interactions, spectral, DNA-binding, docking and subsequent thermolysis to NiO nanocrystals. *J. Mol. Liq.* **2020**, *315*, 113756–113760. [[CrossRef](#)]
39. Al-Zaqri, N.; Salih, K.S.M.; Awwadi, F.F.; Alsalmeh, A.; Alharthi, F.A.; Alsyahi, A.; Ali, A.A.; Zarrouk, A.; Aljohani, M.; Chetouni, A.; et al. Synthesis, physicochemical, thermal, and XRD/HSA interactions of mixed [Cu(Bipy)(Dipn)](X)₂ complexes: DNA binding and molecular docking evaluation. *J. Coord. Chem.* **2020**, *73*, 3236–3248. [[CrossRef](#)]
40. Badran, I.; Tighadouini, S.; Radi, S.; Zarrouk, A.; Warad, I. Experimental and first-principles study of a new hydrazine derivative for DSSC applications. *J. Mol. Struct.* **2021**, *1229*, 129799. [[CrossRef](#)]
41. Saleemh, F.; Musameh, S.; Sawafta, A.; Brandao, P.; Tavares, C.J.; Ferdov, S.; Barakat, A.; Ali, A.A.; Al-Noaimi, M.; Warad, I. Diethylenetriamine/diamines/copper (II) complexes [Cu(dien)(NN)]Br₂: Synthesis, solvatochromism, thermal, electrochemistry, single crystal, Hirshfeld surface analysis and antibacterial activity. *Arab. J. Chem.* **2017**, *10*, 845–854. [[CrossRef](#)]
42. Boshala, A.; Abraham, A.; Almughery, A.; Al-Zaqri, N.; Zarrouk, A.; Lgaz, H.; Warad, I. Spectroscopic Insight into Tetrahedrally Distorted Square Planar Copper(II) Complex: XRD/HSA, Physicochemical, DFT, and Thermal Investigations. *Crystals* **2021**, *11*, 1179. [[CrossRef](#)]
43. Hijji, Y.; Rajan, R.; Ben Yahia, H.; Mansour, S.; Zarrouk, A.; Warad, I. One-Pot Microwave-Assisted Synthesis of Water-Soluble Pyran-2,4,5-triol Glucose Amine Schiff Base Derivative: XRD/HSA Interactions, Crystal Structure, Spectral, Thermal and a DFT/TD-DFT. *Crystals* **2021**, *11*, 117. [[CrossRef](#)]
44. Alsimaree, A.; Alsenani, N.; Alatawi, O.; AlObaid, A.; Knight, J.G.; Messali, M.; Zarrouk, A.; Warad, I. π -Extended Boron Difluoride [N \bar{N} NBF₂] Complex, Crystal Structure, Liquid NMR, Spectral, XRD/HSA Interactions: A DFT and TD-DFT Study. *Crystals* **2021**, *11*, 606. [[CrossRef](#)]
45. Titi, A.; Almutairi, S.; Touzani, R.; Messali, M.; Tillard, M.; Hammouti, B.; El Kodadi, M.; Eddikee, D.; Zarrouk, A.; Warad, I. A new mixed pyrazole-diamine/Ni(II) complex, Crystal structure, physicochemical, thermal and antibacterial investigation. *J. Mol. Struct.* **2021**, *1236*, 130304–130310. [[CrossRef](#)]
46. Barakat, A.; Al-Noaimi, M.; Suleiman, M.; Aldwayyann, A.; Hammouti, B.; Ben Hadda, T.; Haddad, S.; Boshala, A.; Warad, I. One step Synthesis of NiO nanoparticles via solid-state thermal decomposition at low-temperature of novel aqua(2,9-dimethyl-1,10-phenanthroline)NiCl₂ complex. *I. Int. J. Mol. Sci.* **2013**, *14*, 23941–23954. [[CrossRef](#)]